

Differentiation between dysplastic nodule and early-stage hepatocellular carcinoma: The utility of conventional MR imaging

Chen-Te Chou, Jung-Mao Chou, Ting-An Chang, Shiu-Feng Huang, Chia-Bang Chen, Yao-Li Chen, Ran-Chou Chen

Chen-Te Chou, Ran-Chou Chen, Department of Biomedical Imaging and Radiological Science, National Yang-Ming Medical University, Taipei 112, Taiwan

Chen-Te Chou, Chia-Bang Chen, Department of Radiology, Chang-Hua Christian Hospital, Chang-Hua 500, Taiwan

Jung-Mao Chou, Ting-An Chang, Shiu-Feng Huang, Department of Pathology, Taipei City Hospital, Taipei 106, Taiwan

Yao-Li Chen, Transplant Medicine and Surgery Research Centre, Chang-Hua Christian Hospital, Chang-Hua 500, Taiwan

Ran-Chou Chen, Department of Radiology, Taipei City Hospital, Taipei 106, Taiwan

Author contributions: Chou CT and Chen RC designed the research; Chou CT, Chen CB, Chou JM, Chang TA, and Huang SF performed the research; Chen RC and Chen YL analyzed the data; and Chou CT, Chou JM and Chen RC wrote the manuscript.

Correspondence to: Ran-Chou Chen, MD, Department of Biomedical Imaging and Radiological Science, National Yang-Ming Medical University, Beitou District, Taipei 112, Taiwan. chenranchou@yahoo.com.tw

Telephone: +886-2-27093600-5103 Fax: +886-2-27040013

Received: June 22, 2013

Revised: August 16, 2013

Accepted: September 16, 2013

Published online: November 14, 2013

Abstract

AIM: To elucidate the variety of ways early-stage hepatocellular carcinoma (HCC) can appear on magnetic resonance (MR) imaging by analyzing T1-weighted, T2-weighted, and gadolinium-enhanced dynamic studies.

METHODS: Seventy-three patients with well-differentiated HCC (wHCC) or dysplastic nodules were retrospectively identified from medical records, and new histological sections were prepared and reviewed. The tumor nodules were categorized into three groups: dysplastic nodule (DN), wHCC compatible with Edmondson-Steiner grade I HCC (w1-HCC), and wHCC compatible with

Edmondson-Steiner grade II HCC (w2-HCC). The signal intensity on pre-contrast MR imaging and the enhancing pattern for each tumor were recorded and compared between the three tumor groups.

RESULTS: Among the 73 patients, 14 were diagnosed as having DN, 40 were diagnosed as having w1-HCC, and 19 were diagnosed as having w2-HCC. Hyperintensity measurements on T2-weighted axial images (T2WI) were statistically significant between DNs and wHCC ($P = 0.006$) and between DN and w1-HCC ($P = 0.02$). The other imaging features revealed no significant differences between DN and wHCC or between DN and w1-HCC. Hyperintensity on both T1W out-phase imaging ($P = 0.007$) and arterial enhancement on dynamic study ($P = 0.005$) showed statistically significant differences between w1-HCC and w2-HCC. The other imaging features revealed no significant differences between w1-HCC and w2-HCC.

CONCLUSION: In the follow-up for a cirrhotic nodule, increased signal intensity on T2WI may be a sign of malignant transformation. Furthermore, a noted loss of hyperintensity on T1WI and the detection of arterial enhancement might indicate further progression of the histological grade.

© 2013 Baishideng Publishing Group Co., Limited. All rights reserved.

Key words: Dysplastic nodule; Hepatocellular carcinoma; Histological grading; Magnetic resonance imaging; Well-differentiated hepatocellular carcinoma

Core tip: The aim of this article was to differentiate between early-stage hepatocellular carcinoma (HCC) and dysplastic nodules using conventional magnetic resonance (MR) imaging. We found that conventional MR imaging could provide additional information to dif-

ferentiate between early-stage HCC and dysplastic nodules in equivocal lesions. During follow-up for a cirrhotic nodules, increased signal intensity on T2-weighted axial images may be a sign of malignant transformation. Loss of hyperintensity on T1WI and the detection of arterial enhancement may indicate further progression of the histological grade.

Chou CT, Chou JM, Chang TA, Huang SF, Chen CB, Chen YL, Chen RC. Differentiation between dysplastic nodule and early-stage hepatocellular carcinoma: The utility of conventional MR imaging. *World J Gastroenterol* 2013; 19(42): 7433-7439 Available from: URL: <http://www.wjgnet.com/1007-9327/full/v19/i42/7433.htm> DOI: <http://dx.doi.org/10.3748/wjg.v19.i42.7433>

INTRODUCTION

Hepatocellular carcinoma (HCC) is one of the most commonly diagnosed malignant tumors in the world. HCC occurs primarily in patients with chronic liver disease such as hepatitis B and C infections^[1,2]. HCC develops by means of a multi-step dedifferentiation process that progresses from regenerative nodule to dysplastic nodule (DN) and then to HCC^[3]. Early detection of HCC in cirrhotic livers is important to improve patient outcomes and decision-making to determine optimum therapeutic strategies^[4]. A follow-up system for high-risk HCC populations has been established. Additionally, research and technology have enabled increasing numbers of small nodular lesions to be detected. According to the practice guidelines of the American Association for the Study of Liver Diseases (AASLD), HCC can be diagnosed noninvasively in at-risk patients, who typically demonstrate arterial-phase enhancement and venous- or delayed-phase washout on dynamic computed tomography (CT) or magnetic resonance imaging (MRI)^[5]. However, most of these nodules with characteristic CT or MR patterns are overt HCC. The percentage of well-differentiated HCCs showing typical hypervascularity in the arterial-phase followed by washout in the delayed-phase on a dynamic study ranges from 13% to 50%^[6,7]. Therefore, well-differentiated HCCs are increasingly detected in our daily practice, yet many represent diagnostic difficulties.

Gadoxetic acid (Gd-EOB-DTPA)-enhanced MRI has been demonstrated to be useful in differentiating between early HCC and dysplastic nodules in several recent studies^[8,9]. However, the overlap between dysplastic nodules and HCC on gadoxetic acid-enhanced MR presentations has also been mentioned in the literature^[10,11]. Due to the facts that gadoxetic acid is not available in every country and is costly, conventional MRI remains an important tool in differentiating between cirrhotic nodules and early HCC. Conventional MR imaging protocols rely on T1-weighted and T2-weighted imaging and multiphase dynamic gadolinium-enhanced imaging to depict and characterize tumors^[12,13]. To the best of our knowledge,

the role of conventional MR sequences in differentiating between early-stage HCC and dysplastic nodule in cirrhotic liver has not yet been established. The purpose of our study was to elucidate the variety ways of early-stage HCC can appear on MR imaging by analyzing T1-weighted, T2-weighted, and gadolinium-enhanced dynamic studies.

MATERIALS AND METHODS

Patient population

Approval for this retrospective study was obtained from the institutional review board of our hospital. A flow-chart for the patient selection process is shown in Figure 1. Ultimately, 73 patients (51 men and 22 women; mean age, 61 years old; range, 26-82 years) were enrolled in this study. Among them, 70 patients underwent liver biopsy, and 3 patients underwent hepatectomy. All 73 patients had liver cirrhosis: 29 patients had hepatitis B virus; 28 patients had hepatitis C virus; 9 patients had hepatitis B and C co-infections; and 7 patients had alcoholic cirrhosis. Among the 73 patients, 49 patients had Child-Pugh class A cirrhosis, and 24 patients had Child-Pugh class B cirrhosis. The diagnoses of liver cirrhosis were all based on histopathological examination.

Histopathological diagnosis

New histological sections from the original paraffin blocks of all 73 patients' liver tumors were prepared using hematoxylin and eosin stain. The diagnostic features for HCC included the following: (1) increased cell density >2 times the density of the surrounding tissue, with an increased nuclear:cytoplasmic ratio; (2) thickened liver cell plates (2 cells or more); (3) pseudoglandular structure formations; (4) unpaired arteries; (5) sinusoidal capillarization; and (6) stromal invasion without ductular reaction at the periphery of the nodules^[14,15]. Immunohistochemical stains for CD10 (Biocare Medical, Concord, CA, United States), CD34 (DAKO, Glostrup, Denmark) and cytokeratin 7 (DAKO, Glostrup, Denmark) were also performed to facilitate interpretation. The tumor nodules were categorized into three groups: DN, well-differentiated HCC compatible with Edmondson-Steiner grade I HCC (w1-HCC)^[16], and well-differentiated HCC compatible with Edmondson-Steiner grade II HCC [which also included well-differentiated HCC in the World Health Organization system (w2-HCC)^[17].

Two pathologists with more than 10 years of experience in hepatic pathology reviewed all the histological sections independently. Differences between the two reviewers were resolved by a third pathologist to reach a final consensus. All three of the pathologists were blinded to the original pathology diagnoses and the clinical information.

The presence of high cellularity, diffuse capillarization, abnormal biliary canaliculi and stromal invasion were considered features of w1-HCC. The additional presence of nuclear pleomorphism and thicker trabecular growth further upgraded a lesion to, w2-HCC.

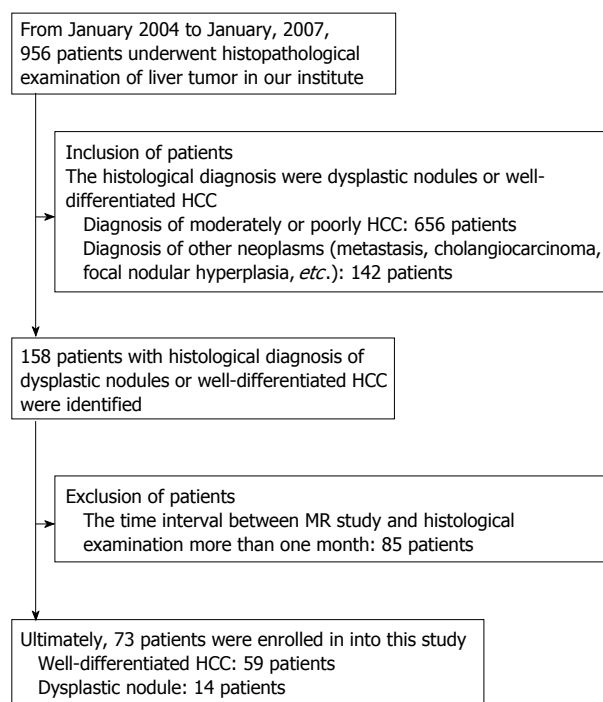


Figure 1 Flowchart of the patient selection process. HCC: Hepatocellular carcinoma; MR: Magnetic resonance.

MR imaging

MR imaging of livers was performed using a 1.5-T MR scanner (Philips Gyroscan ACS-NT Powertrak 6000, release version 6.7.2, Best, the Netherlands) and a phased-array body coil. Turbo spin-echo (TSE) T2-weighted axial images [T2WI, TR/TE: 2500/90 ms, slice thickness/gap: 8/0.8 mm, matrix: 192×256 , number of average (NEX): 2, TSE factor: 23, field of view (FOV): 38-40 cm, typical scanning time: 2 min 20 s] with and without fat saturation (FS, spectral fat saturation inversion recovery) and coronal T2-weighted images were obtained under respiratory trigger. Dual-echo T1-weighted imaging (TR/TE: 210/2.3 ms and 4.6 ms, slice thickness/gap: 8/0.8 mm, matrix: 192×256 , NEX: 1, FOV: 38-40 cm, typical scanning time: 24 s) was also performed during one breath hold. Automatic shimming was applied for fat-suppression imaging to maximize magnetic field homogeneity, and flow compensation was also used.

For contrast-enhanced MR imaging, gadodiamide (Omniscan, GE Healthcare, Oslo, Norway) was administered by bolus injection (approximate rate of 2 mL/s) through a peripheral vein at a dosage of 0.1 mmol/kg. Dynamic T1-weighted fast field echo imaging (175-210/1.3-2.1, flip angle: 80° , matrix: 192×256 , NEX: 1, FOV: 38-40 cm) was performed just before, 18-20 s after and 50-55 s after the contrast agent was injected. An equilibrium phase FS-T1W (TR/TE 241-344/2.7 ms, flip angle: 70° , slices thickness/gap: 8/0.8 mm) imaging was performed 180 s after the contrast agent injection.

Imaging analysis

The imaging analysis was performed at a dual-screen

diagnostic workstation (GE Healthcare, Milwaukee, WI, United States). In each image assessment, liver maps were completed by drawing each individual liver lesion on a respective map according to the Couinaud system of liver anatomy. These drawings were made as accurately as possible by one investigator. All the imaging results were analyzed using visual assessment by two radiologists who each had more than 10 years of experience in abdominal MR imaging. The two observers were blinded to the clinical information and final diagnoses, and they recorded the lesion signal intensities on pre-contrast T1WI and T2WI, post-contrast T1WI and the enhancement pattern during dynamic study. The signal intensity of the focal liver nodule on dual-echo T1WI and T2WI was classified as hypointense, isointense, or hyperintense compared with adjacent liver parenchyma. The enhancement pattern of the HCC was visually classified into one of the following patterns: hypovascular, isovascular or hypervascular enhancement compared with the adjacent liver parenchyma. Any disagreements between the two reviewers were resolved by consensus with a third radiologist who was also blinded to the clinical information and final diagnoses.

Statistical analysis

The interobserver agreement was evaluated using the kappa statistic^[18]. Continuous variables such as age, tumor size, and alpha-fetoprotein were analyzed using the Kruskal-Wallis test. Categorical variables such as signal intensity and enhancement pattern were analyzed using Pearson's χ^2 test. The diagnostic performance of the HCC diagnostic criteria was evaluated along with a receiver operating characteristic analysis. A *P* value less than 0.05 was considered statistically significant.

RESULTS

Among the 73 patients in our study, 14 were diagnosed with a DN, 40 were diagnosed with w1-HCC, and 19 were diagnosed with w2-HCC. The clinicopathological characteristics of the growths are shown in Table 1, which shows no significant differences between the three patient groups. The interobserver agreement for the imaging analysis between the two radiologists was either good or excellent (Table 2).

Univariate analyses of MR findings for patients with DNs and wHCC are shown in Table 3. Only a hyperintense signal on T2WI was a statistically significant predictor of wHCC ($P = 0.006$), whereas the other imaging features revealed no significant associations with DN and wHCC. Therefore, well-differentiated HCCs were divided into w1-HCC and w2-HCC, and the differences between DN *vs* w1-HCC and w1-HCC *vs* w2-HCC were analyzed. Only hyperintensity on T2WI was a statistically significant differentiator of DN from w1-HCC ($P = 0.02$). The other imaging features revealed no significant differences between DN and w1-HCC. Hyperintensity on T1W out-phase imaging ($P = 0.007$) and arterial enhancement on dynamic study ($P = 0.005$) showed statistically significant

Table 1 Clinical characteristics of the 73 cirrhotic patients with liver nodules

	Histopathological diagnosis			P value
	DN (n = 14)	w1-HCC (n = 40)	w2-HCC (n = 19)	
Age (mean ± SD, yr)	54.9 ± 12.9	62.4 ± 12.2	63.4 ± 10.8	0.129
Sex				0.629
Male	11	27	12	
Female	3	13	7	
Underlying liver disease				0.640
HBV	7	15	7	
HCV	3	15	10	
HBV + HCV	2	6	1	
Alcoholism	2	4	1	
Child-Pugh class				0.645
A	10	25	14	
B	4	15	5	
Tumor size (mean ± SD, cm)	1.8 ± 0.6	2.1 ± 0.7	2.9 ± 2.3	0.365
AFP (mean ± SD, ng/mL)	17.1 ± 27.9	55.5 ± 117.9	64.2 ± 169.7	0.202
< 20 ng/mL	12	28	13	0.790
≥ 20 ng/mL	2	12	6	
> 20, ≤ 100 ng/mL	2	7	4	
> 100, ≤ 200 ng/mL	0	0	1	
> 200 ng/mL	0	5	1	

HBV: Hepatitis B virus; HCV: Hepatitis C virus; AFP: Alpha-fetal protein; DN: Dysplastic nodule; w1-HCC: Well-differentiated hepatocellular carcinoma compatible with Edmondson-Steiner grade I; w2-HCC Well-differentiated hepatocellular carcinoma compatible with Edmondson-Steiner grade II.

differences between w1-HCC and w2-HCC. However, T2WI and other imaging sequences showed no significant differences between w1-HCC and w2-HCC.

Using hyperintensity on T2WI as the sole criteria in differentiating wHCC from a dysplastic nodule, 25 of 59 wHCCs could be correctly diagnosed. The sensitivity, specificity, positive predictive value (PPV) and negative predictive value (NPV) were 42%, 93%, 96% and 28%, respectively. Solely using the AASLD criteria (arterial enhancement followed by washout on dynamic imaging) to differentiate between wHCC and dysplastic nodules, only 9 of 59 wHCCs (w1-HCC: 2, w2-HCC: 7) were correctly diagnosed. The sensitivity, specificity, PPV and NPV were 15%, 93%, 90% and 21%, respectively. If the diagnostic criteria were changed to either a hyperintense nodule on T2WI or a lesion that demonstrated arterial enhancement followed by washout on dynamic imaging, 27 of 59 wHCCs were correctly diagnosed. The sensitivity, specificity, PPV, and NPV were 46%, 86%, 93%, and 27%, respectively. Eighteen wHCCs were further detected by the additional hyperintense-on-T2WI criterion according to the AASLD criteria. The diagnostic performance of the AASLD criteria with additional hyperintense findings on T2WI was superior to the AASLD criteria alone in the characterization of early-stage HCC ($P = 0.013$).

DISCUSSION

The development of HCC in the cirrhotic liver is de-

Table 2 Interobserver agreement for magnetic resonance features

MR features	k value
T1-weighted in-phase imaging	0.853
T1-weighted opposed-phase imaging	0.870
Fatty metamorphosis	0.819
T2-weighted imaging	0.828
Arterial enhancement	0.806
Late-phase T1-weighted imaging	0.743

MR: Magnetic resonance.

scribed as either *de novo* hepatocarcinogenesis or as the result of a multistep progression. The stages of the multistep progression originate from a dysplastic nodule, which progresses to a dysplastic nodule with HCC foci, followed by a small HCC, and finally to an overt carcinoma^[19,20]. In our study, typical arterial enhancing features were only detected in 12 (12/40) w1-HCCs, and there were no significant differences between DN and w1-HCC. In contrast, the arterial enhancing feature was demonstrated in 13 (13/19) w2-HCCs and showed a statistically significant difference between w1-HCC and w2-HCC ($P = 0.005$). Our results might explain why the percentage of well-differentiated HCCs with arterial enhancement ranges from 43% to 66% in the current literature^[21-23]. These figures may have resulted from the varied compositions of w1-HCC and w2-HCC within the studies.

The arterial enhancement during dynamic study showed a statistically significant difference between w1-HCC and w2-HCC in our study. This finding might be due to the insufficient development of non-triadal arteries in early-stage HCCs^[14,24]. Kojiro^[25] also reported that early HCCs tended to demonstrate histological hypovascularity. Kim *et al*^[26] reported that the histological grade of HCC was an important factor influencing therapeutic results. They further suggested that treatment could be more effective after radiofrequency ablation in patients with histologically low-grade HCC. According to our results, wHCC demonstrated arterial enhancement during dynamic study, and the histological differentiation tended to be of a higher grade, so it should be treated aggressively.

In our results, only 9 wHCCs (15%) satisfied the AASLD HCC diagnostic criteria. In contrast, T2WI hyperintensity was the only imaging feature that allowed differentiation between wHCC and DN or w1-HCC and DN. The diagnostic performance of the AASLD criteria with additional hyperintensity on T2WI was superior to the AASLD criteria alone in the characterization of early-stage HCCs ($P = 0.013$). Ouedraogo *et al*^[27] also reported that adding T2W hyperintensity to the AASLD criteria increased the detection of HCC, especially in nodules smaller than 20 mm. According to our results, hyperintensity on T2WI alone could offer additional information in dynamic studies to differentiate between wHCC and DN, and a cirrhotic nodule that is hyperintense on

Table 3 Comparison of magnetic resonance features between dysplastic nodule and well-differentiated hepatocellular carcinoma

	DN (n = 14)	wHCC		P value		
		w1 (n = 40)	w2 (n = 19)	DN vs wHCC	DN vs w1	w1 vs w2
In-phase T1WI						
Hyperintense	8	29	8	0.469	0.405	0.074
Isointense	4	5	4			
Hypointense	2	6	7			
Opposed-phase T1WI				0.661	0.565	0.007
Hyperintense	8	25	4			
Isointense	3	4	6			
Hypointense	3	11	9			
Fatty metamorphosis				0.192	0.311	0.450
Positive	0	5	4			
Negative	14	35	15			
T2WI				0.006	0.020	0.109
Hyperintense	1	14	12			
Isointense	6	5	2			
Hypointense	7	21	5			
Arterial enhancement				0.767	0.753	0.005
Hypervascular	5	12	13			
Iso-/hypo-vascular	9	28	6			
Late-phase T1WI				0.112	0.286	0.105
Hyperintense	1	5	3			
Isointense	12	26	7			
Hypointense	1	9	9			

T1WI: T1-weighted imaging; T2WI: T2-weighted imaging; DN: Dysplastic nodule; wHCC: Well-differentiated hepatocellular carcinoma; w1: wHCC compatible with Edmondson-Steiner grade I; w2: wHCC compatible with Edmondson-Steiner grade II.

T2WI should be aggressively biopsied.

In our study, hyperintensity on T1W out-phase imaging showed a significant difference between w1-HCC and w2-HCC. A hyperintense HCC on unenhanced T1W images tended to be lower grade histologically. This finding might be because borderline lesions and some early HCCs/wHCCs are occasionally hyperintense on unenhanced T1W images^[28,29]. Matsui *et al.*^[30] correlated MR signal intensity with tumor histology, and considered cell crowding, fatty accumulation and possibly copper deposition to be responsible for the hyperintensity on T1W imaging. However, the exact histological composition responsible for the signal intensity characteristics of w1-HCC and w2-HCC remains elusive.

According to the step-wise carcinogenesis model, HCC changes in appearance through the course of its development. These changes include a steadily increasing signal intensity on T2WI with gradually increasing neovascularity in most lesions. Van den Bos *et al.*^[31] suggested that the increased signal on T2W images lags behind the developing neovascularity. Our results supported the proposition that an increased signal on T2W images occurs early in the developing arterial enhancement. These discrepancies in enhancement patterns and signal intensities might be due to the different patient populations being examined and the different underlying liver diseases. However, more studies are needed for a better understanding of developing HCC using MR imaging.

Recent progress in CT angiography, Gd-EOB-DTPA-enhanced MRI, diffusion-weighted imaging (DWI), contrast-enhanced ultrasound (CEUS) has made these modalities useful in differentiating HCC from dysplastic

nodules. Lee *et al.*^[11] reported that hypointensity on Gd-EOB-DTPA-enhanced hepatobiliary-phase images and hyperintensity on high-b-value DWI in the surrounding liver parenchyma were useful in differentiating wHCC from benign nodules. Kudo^[3] reported that CT during hepatic angiography and CT during arterial portography were the most sensitive tools in differentiating between premalignant/borderline lesions and early HCC. Real-time CEUS has the ability to detect slowly enhancing HCCs, which on CT could be interpreted as hypovascular lesions^[32]. Giorgio *et al.*^[33] reported that DN, early HCC and progressed HCC could be accurately differentiated using CEUS on the basis of the vascularization pattern during the arterial phase. Kudo^[34] reported that Sonazoid-enhanced US could generate both hemodynamic-phase and Kupper-phase images and offer improved diagnostic performance for focal liver lesions. CEUS with Sonazoid may play an important role in the characterization of focal hepatic lesions in the future.

This study had two main limitations. First, the study was retrospective. If we had used the original pathological reports in the medical records as a standard of reference, inaccuracies due to differing standards of pathological interpretation at that time might have led to different results. To ensure accurate histological diagnoses, new histological slides were prepared from paraffin-embedded blocks, all of which were read by two experienced pathologists independently. A third pathologist was involved as needed to reach a final consensus when disagreements arose. The second limitation was that the histological diagnoses of 70 of the nodules (70/73) were based on needle biopsies. Potential sampling errors and

sampling variation are inherent in this type of examination, and they are recognized shortcomings in most comparative studies.

In conclusion, conventional MR imaging could provide additional information to differentiate between wHCC and DN in equivocal lesions. The variable presentation of wHCC in the current literature may be due to the differing cellular compositions of w1-HCC and w2-HCC. Consequently, during follow-up of a cirrhotic nodule, increased signal intensity on T2WI may be a sign of malignant transformation. Loss of hyperintensity in T1WI and the detection of arterial enhancement may indicate further progression of the histological grade.

COMMENTS

Background

Most well-differentiated hepatocellular carcinomas (HCCs) at an early stage do not demonstrate hypervascularity upon dynamic computed tomography/magnetic resonance (CT/MR) study, thereby making their diagnosis difficult. Some well-differentiated HCCs are fed by the portal vein instead of the hepatic artery and may look like benign nodules with "benign-appearing" patterns of vasculature. Gadoteric acid-enhanced magnetic resonance imaging (MRI) and contrast-enhanced ultrasound have been demonstrated to be useful in differentiating between early-stage HCC and dysplastic nodules in several recent studies. Due to the facts that gadoteric acid and contrast medium for ultrasound are not available in every country and are costly, conventional MRI remains an important tool in differentiating between cirrhotic nodules and early HCCs. The authors used a retrospective analysis to show the utility of MR imaging features to differentiate between dysplastic nodules and early stage HCC.

Research frontiers

The authors compared conventional MR imaging results with histological results to evaluate the effectiveness of conventional MR imaging in the diagnosis of early-stage HCC.

Innovations and breakthroughs

Increased signal intensity on T2-weighted axial images (T2WI) may be a sign of malignant transformation. Loss of hyperintensity on T1-weighted axial images (T1WI) and the detection of arterial enhancement may indicate further progression of the histological grade.

Applications

The authors believe that conventional MR imaging could provide additional information in differentiating between early-stage HCC and dysplastic nodule in equivocal lesions. During follow-up for a cirrhotic nodule, increased signal intensity on T2WI may be a sign of malignant transformation and should be biopsied. Loss of hyperintensity on T1WI and the detection of arterial enhancement may indicate further progression of the histological grade and should be treated aggressively.

Peer review

The authors describe a retrospective analysis of 73 patients with well-differentiated HCC or dysplastic nodules. The authors address the question whether MR imaging is helpful to differentiate between a dysplastic nodules and well-differentiated HCC in high-risk patients with cirrhosis. The question addressed by the authors is of high impact in the field of liver cirrhosis. Despite the limitations of the study (retrospective analysis, 73 patients), the authors have thoroughly analyzed the data and have made new histological classifications of all the specimens. The data show that increased signal intensity on T2WI may be a sign of malignant transformation.

REFERENCES

- 1 **Parkin DM**, Bray F, Ferlay J, Pisani P. Global cancer statistics, 2002. *CA Cancer J Clin* 2005; **55**: 74-108 [PMID: 15761078 DOI: 10.3322/canjclin.55.2.74]
- 2 **Donato F**, Tagger A, Chiesa R, Ribero ML, Tomasoni V, Fasola M, Gelatti U, Portera G, Boffetta P, Nardi G. Hepatitis B and C virus infection, alcohol drinking, and hepatocellular carcinoma: a case-control study in Italy. *Brescia HCC Study. Hepatology* 1997; **26**: 579-584 [PMID: 9303486 DOI: 10.1002/hep.510260308]
- 3 **Kudo M**. Multistep human hepatocarcinogenesis: correlation of imaging with pathology. *J Gastroenterol* 2009; **44** Suppl 19: 112-118 [PMID: 19148804 DOI: 10.1007/s00535-008-2274-6]
- 4 **Szklaruk J**, Silverman PM, Charnsangavej C. Imaging in the diagnosis, staging, treatment, and surveillance of hepatocellular carcinoma. *AJR Am J Roentgenol* 2003; **180**: 441-454 [PMID: 12540450 DOI: 10.2214/ajr.180.2.1800441]
- 5 **Bruix J**, Sherman M. Management of hepatocellular carcinoma: an update. *Hepatology* 2011; **53**: 1020-1022 [PMID: 21374666 DOI: 10.1002/hep.24199]
- 6 **Yoon SH**, Lee JM, So YH, Hong SH, Kim SJ, Han JK, Choi BI. Multiphasic MDCT enhancement pattern of hepatocellular carcinoma smaller than 3 cm in diameter: tumor size and cellular differentiation. *AJR Am J Roentgenol* 2009; **193**: W482-W489 [PMID: 19933622 DOI: 10.2214/AJR.08.1818]
- 7 **Li CS**, Chen RC, Tu HY, Shih LS, Zhang TA, Lii JM, Chen WT, Duh SJ, Chiang LC. Imaging well-differentiated hepatocellular carcinoma with dynamic triple-phase helical computed tomography. *Br J Radiol* 2006; **79**: 659-665 [PMID: 16641423 DOI: 10.1259/bjr/12699987]
- 8 **Kudo M**. The 2008 Okuda lecture: Management of hepatocellular carcinoma: from surveillance to molecular targeted therapy. *J Gastroenterol Hepatol* 2010; **25**: 439-452 [PMID: 20370723 DOI: 10.1111/j.1440-1746.2009.06207.x]
- 9 **Okada M**, Imai Y, Kim T, Kogita S, Takamura M, Kumano S, Onishi H, Hori M, Fukuda K, Hayashi N, Wakasa K, Sakamoto M, Murakami T. Comparison of enhancement patterns of histologically confirmed hepatocellular carcinoma between gadoxetate- and ferucarbotran-enhanced magnetic resonance imaging. *J Magn Reson Imaging* 2010; **32**: 903-913 [PMID: 20882621 DOI: 10.1002/jmri.22333]
- 10 **Kogita S**, Imai Y, Okada M, Kim T, Onishi H, Takamura M, Fukuda K, Igura T, Sawai Y, Morimoto O, Hori M, Nagano H, Wakasa K, Hayashi N, Murakami T. Gd-EOB-DTPA-enhanced magnetic resonance images of hepatocellular carcinoma: correlation with histological grading and portal blood flow. *Eur Radiol* 2010; **20**: 2405-2413 [PMID: 20490505 DOI: 10.1007/s00330-010-1812-9]
- 11 **Lee MH**, Kim SH, Park MJ, Park CK, Rhim H. Gadoteric acid-enhanced hepatobiliary phase MRI and high-b-value diffusion-weighted imaging to distinguish well-differentiated hepatocellular carcinomas from benign nodules in patients with chronic liver disease. *AJR Am J Roentgenol* 2011; **197**: W868-W875 [PMID: 22021534 DOI: 10.2214/AJR.10.6237]
- 12 **Lee JM**, Choi BI. Hepatocellular nodules in liver cirrhosis: MR evaluation. *Abdom Imaging* 2011; **36**: 282-289 [PMID: 21399975 DOI: 10.1007/s00261-011-9692-2]
- 13 **Willatt JM**, Hussain HK, Adusumilli S, Marrero JA. MR Imaging of hepatocellular carcinoma in the cirrhotic liver: challenges and controversies. *Radiology* 2008; **247**: 311-330 [PMID: 18430871 DOI: 10.1148/radiol.2472061331]
- 14 **Roskams T**, Kojiro M. Pathology of early hepatocellular carcinoma: conventional and molecular diagnosis. *Semin Liver Dis* 2010; **30**: 17-25 [PMID: 20175030 DOI: 10.1055/s-0030-1247129]
- 15 **Hytioglou P**, Park YN, Krinsky G, Theise ND. Hepatic precancerous lesions and small hepatocellular carcinoma. *Gastroenterol Clin North Am* 2007; **36**: 867-87, vii [PMID: 17996795 DOI: 10.1016/j.gtc.2007.08.010]
- 16 **Edmondson HA**, Steiner PE. Primary carcinoma of the liver: a study of 100 cases among 48,900 necropsies. *Cancer* 1954; **7**: 462-503 [PMID: 13160935 DOI: 10.1002/1097-0142(195405)7]
- 17 **Hamilton SR**, Aaltonen LA. World Health Organization Classification of Tumours. Pathology and Genetics of Tumours of the Digestive System. Lyon, France: IARC Press, 2000: 159-172
- 18 **Landis JR**, Koch GG. The measurement of observer agree-

- ment for categorical data. *Biometrics* 1977; **33**: 159-174 [PMID: 843571 DOI: 10.2307/2529310]
- 19 **Coleman WB**. Mechanisms of human hepatocarcinogenesis. *Curr Mol Med* 2003; **3**: 573-588 [PMID: 14527088 DOI: 10.2174/1566524033479546]
 - 20 **Efremidis SC**, Hytiroglou P. The multistep process of hepatocarcinogenesis in cirrhosis with imaging correlation. *Eur Radiol* 2002; **12**: 753-764 [PMID: 11960222 DOI: 10.1007/s00330-001-1142-z]
 - 21 **Jang HJ**, Kim TK, Burns PN, Wilson SR. Enhancement patterns of hepatocellular carcinoma at contrast-enhanced US: comparison with histologic differentiation. *Radiology* 2007; **244**: 898-906 [PMID: 17709836 DOI: 10.1148/radiol.2443061520]
 - 22 **Saitoh S**, Ikeda K, Koida I, Tsubota A, Arase Y, Chayama K, Kumada H. Serial hemodynamic measurements in well-differentiated hepatocellular carcinomas. *Hepatology* 1995; **21**: 1530-1534 [PMID: 7768496 DOI: 10.1016/0270-9139(95)90455-7]
 - 23 **Arita J**, Hasegawa K, Takahashi M, Hata S, Shindoh J, Sugawara Y, Kokudo N. Correlation between contrast-enhanced intraoperative ultrasound using Sonazoid and histologic grade of resected hepatocellular carcinoma. *AJR Am J Roentgenol* 2011; **196**: 1314-1321 [PMID: 21606294 DOI: 10.2214/AJR.10.4310]
 - 24 **Nakashima Y**, Nakashima O, Hsia CC, Kojiro M, Tabor E. Vascularization of small hepatocellular carcinomas: correlation with differentiation. *Liver* 1999; **19**: 12-18 [PMID: 9928760 DOI: 10.1111/j.1478-3231.1999.tb00003.x]
 - 25 **Kojiro M**. Focus on dysplastic nodules and early hepatocellular carcinoma: an Eastern point of view. *Liver Transpl* 2004; **10**: S3-S8 [PMID: 14762831 DOI: 10.1002/lt.20042]
 - 26 **Kim SH**, Lim HK, Choi D, Lee WJ, Kim SH, Kim MJ, Kim CK, Jeon YH, Lee JM, Rhim H. Percutaneous radiofrequency ablation of hepatocellular carcinoma: effect of histologic grade on therapeutic results. *AJR Am J Roentgenol* 2006; **186**: S327-S333 [PMID: 16632696 DOI: 10.2214/AJR.05.0350]
 - 27 **Ouedraogo W**, Tran-Van Nhieu J, Baranes L, Lin SJ, Decaens T, Laurent A, Djabbari M, Pigneur F, Duvoux C, Kobeiter H, Deux JF, Rahmouni A, Luciani A. [Evaluation of noninvasive diagnostic criteria for hepatocellular carcinoma on pretransplant MRI (2010): correlation between MR imaging features and histological features on liver specimen]. *J Radiol* 2011; **92**: 688-700 [PMID: 21819911 DOI: 10.1016/j.jradio.2011.03.020]
 - 28 **Shinmura R**, Matsui O, Kobayashi S, Terayama N, Sanada J, Ueda K, Gabata T, Kadoya M, Miyayama S. Cirrhotic nodules: association between MR imaging signal intensity and intranodular blood supply. *Radiology* 2005; **237**: 512-519 [PMID: 16244260 DOI: 10.1148/radiol.2372041389]
 - 29 **Efremidis SC**, Hytiroglou P, Matsui O. Enhancement patterns and signal-intensity characteristics of small hepatocellular carcinoma in cirrhosis: pathologic basis and diagnostic challenges. *Eur Radiol* 2007; **17**: 2969-2982 [PMID: 17618439 DOI: 10.1007/s00330-007-0705-z]
 - 30 **Matsui O**, Kadoya M, Kameyama T, Yoshikawa J, Arai K, Gabata T, Takashima T, Nakanuma Y, Terada T, Ida M. Adenomatous hyperplastic nodules in the cirrhotic liver: differentiation from hepatocellular carcinoma with MR imaging. *Radiology* 1989; **173**: 123-126 [PMID: 2550995]
 - 31 **van den Bos IC**, Hussain SM, Terkivatan T, Zondervan PE, de Man RA. Stepwise carcinogenesis of hepatocellular carcinoma in the cirrhotic liver: demonstration on serial MR imaging. *J Magn Reson Imaging* 2006; **24**: 1071-1080 [PMID: 17024654 DOI: 10.1002/jmri.20701]
 - 32 **Nicolau C**, Vilana R, Bianchi L, Brú C. Early-stage hepatocellular carcinoma: the high accuracy of real-time contrast-enhanced ultrasonography in the assessment of response to percutaneous treatment. *Eur Radiol* 2007; **17** Suppl 6: F80-F88 [PMID: 18376461]
 - 33 **Giorgio A**, Calisti G, di Sarno A, Farella N, de Stefano G, Scognamiglio U, Giorgio V. Characterization of dysplastic nodules, early hepatocellular carcinoma and progressed hepatocellular carcinoma in cirrhosis with contrast-enhanced ultrasound. *Anticancer Res* 2011; **31**: 3977-3982 [PMID: 22110230]
 - 34 **Kudo M**. Diagnostic imaging of hepatocellular carcinoma: recent progress. *Oncology* 2011; **81** Suppl 1: 73-85 [PMID: 22212940 DOI: 10.1159/000333265]

P- Reviewers: Enomoto N, Hinz S, Singal AK **S- Editor:** Wen LL
L- Editor: A **E- Editor:** Zhang DN





百世登

Baishideng®

Published by **Baishideng Publishing Group Co., Limited**

Flat C, 23/F., Lucky Plaza,

315-321 Lockhart Road, Wan Chai, Hong Kong, China

Fax: +852-65557188

Telephone: +852-31779906

E-mail: bpgoffice@wjgnet.com

<http://www.wjgnet.com>



ISSN 1007-9327



9 771007 932045